25th ABCM International Congress of Mechanical Engineering
October 20-25, 2019, Uberlândia, MG, Brazil

COBEM2019-0932
PRELIMINARY PROJECT OF A CONCENTRATED SOLAR POWER PLANT OF CENTRAL RECEIVER WITH DIRECT GENERATION OF STEAM FOR THE REGION OF GRANDE DOURADOS

Paulo Henrique Teles Coca[1]
Ramon Eduardo Pereira Silva[2]
Federal University of Grande Dourados – UFGD / FAEN / Engenharia de Energia, Rodovia MS-270 (Dourados-Itahum), km 12, Dourados-MS. CEP: 79804-970.
paulo.coca94@gmail.com[1]; ramonsilva@ufgd.edu.br[2]

Abstract. *In the current energy context, where the growing need for energy generation for sustainable way, environmental preservation and the attempt to curb the greenhouse effect that has been intensifying in recent centuries, has increased the demand for alternative and renewable energies such as solar, wind, hydroelectric, biomass and so on. In this context, Brazil, which already has the largest hydroelectric generation in the world, has been developing other technologies, with the production of ethanol, the use of biomass in thermoelectric power plants and the implementation of wind farms. In the field of solar energy, photovoltaic technology have been expanding in the market and solar water heater is already reasonably widespread in residential and commercial buildings in Brazil, but the production of solar energy in large-scale is still scarce in projects and references in Brazil. As a result, this project, proposes to develop a steam power plant with a heat source by a Concentrated Solar Power (CSP) systems for the production of superheated steam. The aim was to develop a Rankine cycle adapted to replace the steam boiler with a solar concentration tower with a reservoir at the top, and install a field of reflecting mirrors (heliostatos) to concentrate the direct radiation from the sun to the reservoir. In addition, the design of all components of the cycle had be carried out, as well as a thermodynamic of the project.*

Keywords: *Concentrated Solar Power, Renewable Energy, Thermoelectric Plants.*

1. INTRODUCTION

Since the industrial revolution and the starting point of the exploration of fossil fuels like mineral coal and oil, in the beginning of nineteenth century, the energy global demand has been following in constant growth. The advent of capitalism as a prevailing economic regime and the beginning of the so-called "consumer society" shortly after World War II resulted in an exponential growth in the world energy demand. With the advances in technology, in the so-called "developed" countries, consumption of goods and services, such as transportation and travel, has grown, which has increased the need for direct and increasing use of more efficient and dense energy sources beyond the oil and gas, such as uranium and other radioactive materials (Farges, 2014).

With the increasing economic and demographic global consumption and consumption has expanded even faster. By the end of the twentieth century this increase in demand and production was made without any collective consciousness of responsibility and environmental preservation. The International Energy Agency (IEA PVPS, 2017) predicted that global energy needs would continue to increase over the next 25 years, despite the economic crisis in developed countries. Because of this, the need for clean and renewable energy generation for both transportation and electricity generation is currently present in international discussions and agreements, such as the Paris agreement at COP21 in 2015 (Badia, 2014).

In this chaotic climatic and environmental context, whose modern society finds itself, the production of energy from renewable sources gains strength as it presents itself to be able to contribute as part of the solution to this global problem. The reducing consumption and more efficient use of energy is another area that has been gaining momentum. Among renewable energy, solar energy is highlighted by its abundance and potential and must fill a significant part of energy needs in the coming decades (Badia, 2014).

The transformation of solar energy into usable energy is divided into three sectors: Solar thermal energy for the production of domestic hot water, photovoltaic (PV) solar energy for electricity generation through the photovoltaic effect and "Concentrated Solar Power" (CSP), which is also known as thermodynamic or heliothermic solar energy.

In according to Farges (2014), the production of electricity from CSP began in the 1980s. The basic principle is to heat up the process fluid through solar radiation focused to obtain high temperatures values at levels similar to industrial

boilers. The thermal energy is converted into mechanical energy in a turbine and then into electrical energy with a generator. In accordance with the author, there are two main types of solar concentrators: the linear and point concentrators. In the linear concentrators, the concentration happens in tubes where a refrigerant circulates. These tubes are in the focal line of reflectors concentrating the solar radiation under it. The main concentrators that work on this principle are parabolic cylindrical and Fresnel concentrators. In the point concentrators: Concentration is performed in a central receiver where the concentrator device follows the sun in the azimuth and elevation axes. This principle is used by parabolic and central receiver (tower) concentrators.

The vast majority of the plants in operation today use parabolic concentration technology, since it is already a thermodynamic solar technology more mature and tested a few years ago. This paper will explain the central receiver type facilities, interconnected to a Rankine cycle steam plant.

2. STATE OF ART

2.1 The Central Receiver System – CRS

The central receiver system (Figure 1), known by the acronym CRS or by Solar Tower, consists of a field of heliostats, which is a set of reflecting mirrors, which are positioned to the ground with the function of concentrating the solar energy in a fixed central receiver, which is a reservoir with a thermal fluid inside, located at the top of a tower. The primary thermal fluid, such as molten salt or air, heat a secondary fluid in a heat exchanger and thereby to operate the thermodynamic cycle. The thermal fluid can be too the water to be used in the direct generation (Direct Steam Generation - DSG), circulating through the receiver, converting solar energy into thermal energy and then into mechanical and electrical energy, respectively, in the turbine and generator (Aneel, 2015).

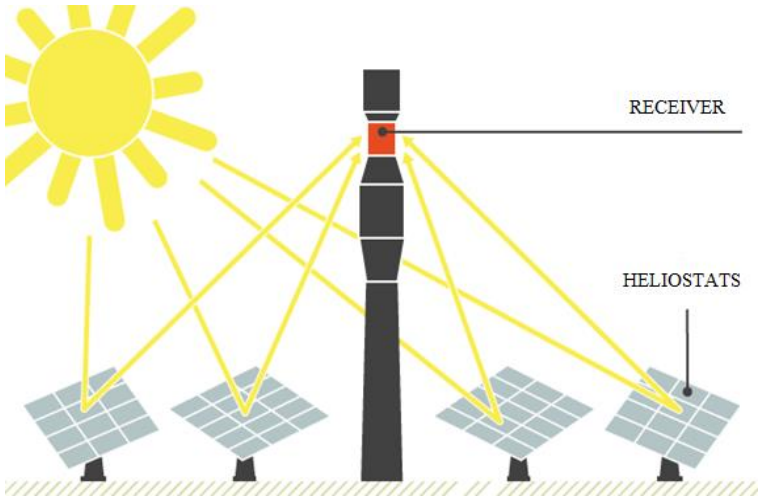

Figure 1. The CSP Central Receiver System or Solar Tower. Source: Portal Solar.

The heliostats (Figure 2) account for up to 40% of the total cost of installation of this type of plant (between US$ 126/m² and US$ 164/m²), due to the surface of mirrors necessary to reach the desired temperatures, reaches tens of thousands of meters squares. Heliostats have areas ranging from 10 m² up to 120 m² and have a useful life of 20-25 years (Eustáquio, 2011).

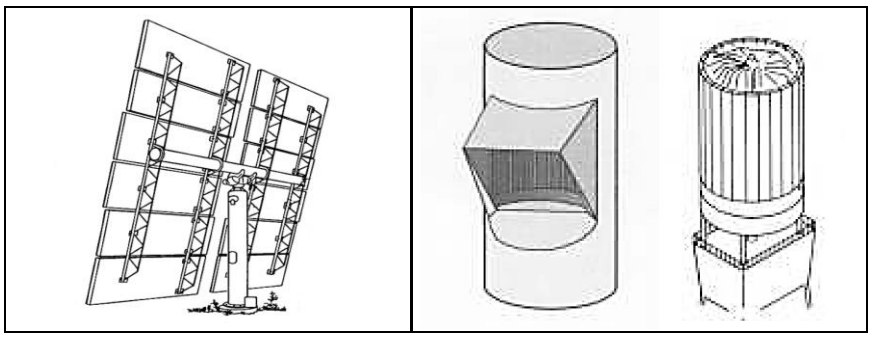

Figure 2. Illustration of a heliostat, a cavity receiver and an external receiver (respectively from left to right). Source: Eustáquio, 2011.

The central receiver, which is at the top of the solar tower, can be of two types: the external and the cavity (Figure 2). In the external receivers, the heat transfer area is totally exposed to the environment, which allows a greater extension of the field of heliostats and flexibility to distribute them. In the cavity receivers, the heat transfer area is inside a cavity, where the entire field of heliostats needs to focus, which limits the field extension and the distribution of the mirrors, in addition to complicating the focus during the day (Bezerra, 2017).

Among the CSP technologies, the CRS is the most recent to be developed. It is a promising technology, since it was the one that presented the highest efficiency in a large-scale generation and could produce steam at temperatures of around 1000°C (Farges, 2014).

2.2 Heliostats Field Design of a CRS system

In accordance with Eustáquio (2011), to size the field of heliostats is necessary to realize the distribution of the mirrors in the determined area. Heliostats need to be concentrated primarily in the region south of the tower (due to the location of the hemisphere) to reflect solar radiation coming from the north, and as close as possible to the tower, the further away, the greater the losses.

The methodology used by Eustáquio (2011), establishes a standard to realize the distribution through the radial and azimuthal distance from heliostats, so that the losses by shading and blocking were minimized. In according to this methodology, the radial and azimuthal distance are defined by Eq. 1 and Eq. 2 and can be seen in Figure 3:

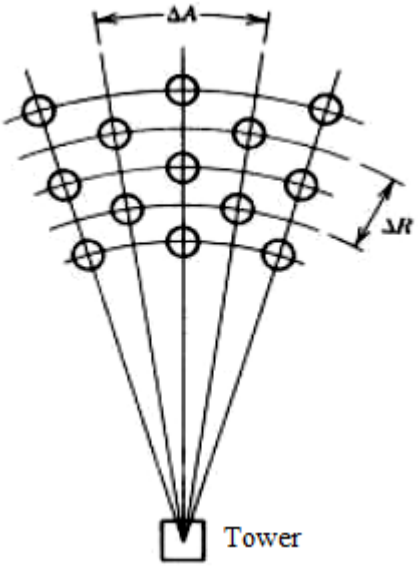

Figure 3. Radial and azimuthal distribution of a heliostat field. Source: Eustáquio, 2011.

$$\Delta R = HM \cdot (1{,}44\,\mathrm{cotg}\,\theta_L - 1{,}094 + 3{,}068\theta_L - 1{,}125\theta_L^2) \tag{1}$$

$$\Delta A = \mathrm{WM} \cdot (1{,}749 + 0{,}6396\theta_L) + \frac{0{,}2873}{\theta_L - 0{,}04902} \tag{2}$$

The *HM* and *MM* are respectively, the height and width of the heliostat. The angle θ_L is the tower height angle from the location of the heliostat field, which is calculated by Eq. 3:

$$\tan\theta_L = \frac{1}{L} \tag{3}$$

The L is distance from the receiver to the heliostat field at "tower height", i.e. if the tower is 100 m high and the heliostat is 200 m away from this tower, for example, its distance L would be equal to 2 tower heights.

According to Eustáquio, the main losses occurring in the field are due to shading (η_{somb}), blocking (η_{bloq}), reflectivity (η_{reflec}), blurring (η_{desf}), attenuation (η_{aten}) and cosine effect (η_{cos}).

The shading occurs when the tower and heliostat shades are over another heliostat, reducing your efficiency. The blocking occurs when one heliostat prevents the radiation flow from another heliostat, reducing your efficiency. In accordance with Eustáquio (2011), the projects that followed the same method of distance cited by the author, reached yields around 97% for shading and blocking.

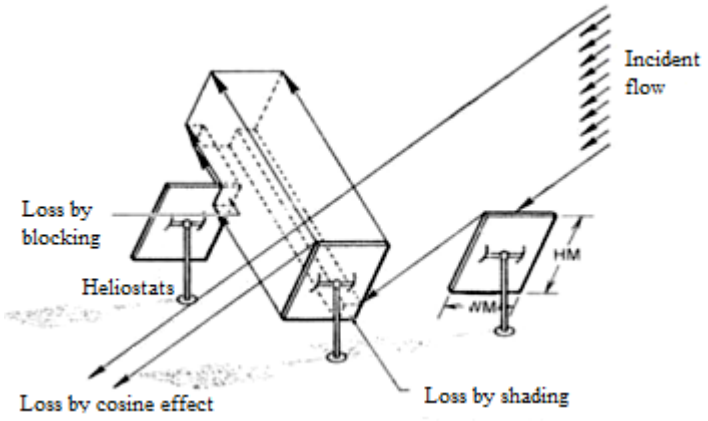

Figure 4. Losses due to shading, blocking and cosine effect. Source: Eustáquio, 2011.

The reflectivity losses depend specifically from mirrors ability to reflect solar radiation and heliostat model used. The current models of mirrors have high efficiency, usually higher than 90% (Eustáquio, 2011).

The blurring is a common loss both to the heliostat and to the receiver, since it refers to the part of radiation that does not reach the absorber surface, either due to the size of the absorber surface or the distance from the mirror to the tower or even to the focus of these. In accordance with Eustáquio (2011) this type of loss is usually in the order of 90% of efficiency, but to determine in detail is necessary, as well as the losses by shading and blocking, the use of specific simulation tools for these types of projects.

The losses due to atmospheric attenuation are the losses of the reflected radiation through the air in the distance traveled from the heliostat to the receiver. How much more distant the heliostat is from the tower, the greater will be this type of loss. The equation to determine the efficiency by atmospheric attenuation (τ_a) depends on the weather conditions, and for the clean sky (Eq. 4) (Eustáquio, 2011):

$$\tau_a = 0{,}99326 - 0{,}1046D + 0{,}017D^2 - 0{,}002845D^3 \quad (4)$$

And for the cloudy and low visibility sky (Eq. 5):

$$\tau_a = 0{,}98707 - 0{,}2748D + 0{,}03394D^2 \quad (5)$$

The *D* is the distance from the heliostat to the receiver in kilometers.

It is important to emphasize that this efficiency must be calculated for each heliostat, since each one has a different distance to the tower, the most distant ones being the least efficient. Thus, the total attenuation efficiency will be the sum of the values of τ_a calculated for each heliostat.

Finally, the losses by cosine effect (Figure 5), which are the largest losses present in the field of heliostats, depend on the position of the sun and the heliostat in relation to the receiver. The heliostat needs that your reflected area to be at the bisection of the angle between the sun's rays and heliostats line to the tower. Thus, the area that is truly reflected by the heliostat is reduced by the cosine effect (Eustáquio, 2011).

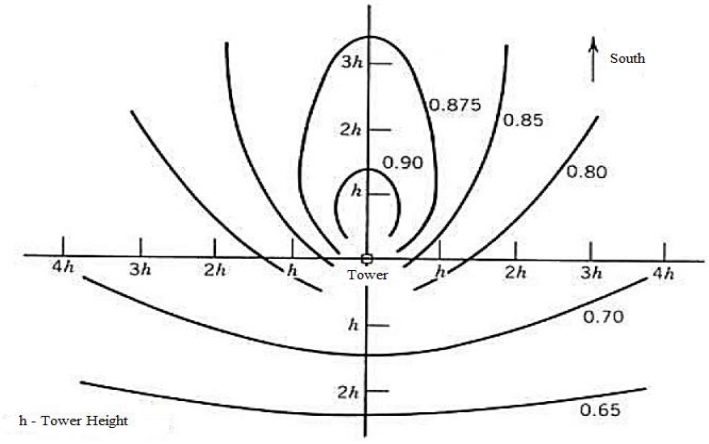

Figure 5. Efficiency of the field of heliostats in relation to the cosine effect. Source: Eustáquio, 2011.

Due to this plant is to be installed in a region in the south hemisphere, the position of the Sun for these regions is to the north and therefore the concentration of heliostats should remain mainly in the south of the tower, so that they can reflect the solar radiation (Eustáquio, 2011). In the case of heliostats, the maximum efficiency in the field of heliostats relative to the cosine effect will also be concentrated to the south of the tower (Eustáquio, 2011). The efficiency is shown in Figure 5, where the h is the distance as a function of the tower height (h = 1 tower height).

After determining all field efficiencies due to recurrent losses, we then have the total heliostat field efficiency (η_{field}) determined by Eq. 6:

$$\eta_{campo} = \eta_{somb} \cdot \eta_{bloq} \cdot \eta_{reflec} \cdot \eta_{desf} \cdot \eta_{aten} \cdot \eta_{cos} \quad (6)$$

The overall efficiency of the heat generation will be the product of the overall efficiency of the heliostats field and the efficiency of the central receiver, which according to Eustáquio (2011). The type of receiver selected for the project is of the external type, so that there is the concentration of radiation coming from all directions. In such plants, the efficiency of the external receiver varies between 85% and 90% (Aneel, 2015). Therefore, the overall efficiency of the heat generator is calculated by Eq. 7:

$$\eta_{global} = \eta_{campo} \cdot \eta_{receptor} \quad (7)$$

The $\eta_{receptor}$ is the efficiency of the central receiver and η_{global} the overall efficiency of the heat generation.

3. METHODOLOGY

The location chosen for this project was the Grande Dourados region in the state of Mato Grosso do Sul. The region has high rates of solar irradiation, mainly between September and February. The region has a latitude of 22°13'18.54 "South, longitude 54°48'23.09" West, altitude of 454 m and a fairly flat terrain.

The solar radiation data of each region of the country is measured in meteorological stations spread in several cities in all the states, realized by centers of research of some universities and research centers like Embrapa. Measurements are carried out using equipment such as pyranometer and pyreliometer. The pyranometer is the instrument that performs the measurements of global radiation, the radiation coming from all directions of the hemispheric plane above the level of the instrument and the pyreliometer is responsible for measuring only the direct radiation, which comes directly from the sun without deviations (Eustáquio, 2011).

The local solar radiation data to be used in this work are from the database of the Solar and Wind Reference Center Sérgio de S. Brito (CRESESB), using local latitude and longitude data. The CRESESB developed the SunData program, which is designed to perform calculations of monthly average daily solar irradiance in any place in the Brazilian territory. The program is an opportunity to offer a tool to support the design of photovoltaic systems.

The SunData database is based on data from the most recent edition (2017) of the Brazilian Solar Energy Atlas, which is the most complete and modern information on solar irradiation in Brazil. The information contained herein is indicative and has the limitations of the models used, that is, for situations where more accurate evaluations are necessary, the measurement of irradiation at the place of interest is recommended. However for this work the database provided is sufficient to meet the expected objectives.

The annual average values recorded by the Dourados 1, 2 and 3 stations were 4.90 kWh/m², 4.92 kWh/m² and 4.88 kWh/m² respectively. For the calculations, the data of the station Dourados 1 were considered, due to the fact that the values were intermediate between the two other stations, despite the low variation.

With the radiation data in hand, initially it is necessary to dimension the thermodynamic cycle so that one knows of the power in heat that will have to be generated in the tower. The selected cycle was a simple steam cycle (Rankine), thus, requiring equipment such as steam turbine, condenser and pump.

There was no merit in detailing the components of the cycle, as well as selecting models in catalogs, since the work focuses only on a preliminary study to evaluate the generation potential for this type of technology in the given region. In this way, the exception was the steam turbine, because its values of admission and exhaustion are necessary to determine important parameters, such as mass flow, power and enthalpy of the thermodynamics states, necessary to the objectives of the work.

Using the parameters of the SIEMENS SST-300 steam turbine model, selected for having a wide power range (10-50 MW), with required temperature and inlet pressure values of 520°C and 120 bar, respectively, and pressure 0.3 bar output.

For this preliminary project, we opted for a generation of approximately 20 MW so as to make a parallel with the work of Eustáquio (2011), which also opted for a generation power of 20 MW (but in the northern hemisphere) and thus use some parameters that he used that are important for the project, such as Tower height (120 m), heliostat surface (100 m²) and shading (97%), blocking (97%), reflection (90%) and blurring (90%) efficiencies. Therefore, it is possible to make a comparative to this work with the obtained results.

Implement the calculations using Microsoft *Excel* software to determine the enthalpy of the 4 thermodynamic states of the cycle and the mass flow, using the thermodynamic tables of Shapiro and Moran (2009), it was possible to determine the power in the turbine and, mainly, the heat generated in the tower (Q_{in}), as it will serve as a reference to dimension the heliostats field.

Heliostat field modeling is undoubtedly the most complex stage of the project, as there are several factors that need to be addressed that directly affect the efficiency of each mirror and generally achieve field efficiency (Eq. 6). Therefore, to model it, it was necessary to use the sequence of equations detailed in State of Art topic 2.2 (Eq. 1-7) and to perform an iterative method until a number of heliostats were determined with an overall efficiency that matched the amount of heat required in the tower (Q_{in}). For these field modeling calculations, *Excel* was also used.

As with every iterative method, it takes an initial guess to start the process, it was decided to consider an overall initial efficiency of 100% and to determine the energy required for the tower, the amount of heliostats under these efficiency conditions and to consider this as the initial guess.

To determine, then, the amount of energy the heat generator needs to receive for the cycle to produce power near 20 MW at 100% heliostat field efficiency, is used in Eq. 8:

$$\dot{Q} = \dot{Q}_{in} = \dot{m}\Delta \mathrm{h} \tag{8}$$

The Q is the required energy flow (power), m is the mass flow of duty fluid and Δh is the specific enthalpy difference of the fluid before and after the solar heating.

With the value of the required power to be transferred to the tower, it was possible to estimate the amount of mirrors required and their respective area. Considering that each heliostat had a surface of 100 m² and having knowledge of the average annual radiation values in the region, it was possible to estimate the necessary surface to reach the amount of heat and the number of mirrors by estimating the ratio between energy and solar radiation flow per square meter (Eq. 9):

$$A_{esp} = \frac{\dot{Q}}{I} \tag{9}$$

Where A_{esp} is the total mirrored area in m² and I is the solar radiation flux in W/m². And then:

$$N_{esp} = \frac{A_{esp}}{A_H} \tag{10}$$

The N_{esp} is the number of mirrors and A_H is the area of each heliostat (Eq. 10). The calculated value will most likely not be an integer, so the final value of N_{esp} should be rounded up to the next integer and use this number for subsequent calculations.

With the value of global efficiency, the iterative method was used, because when global efficiency was used, it would be necessary to increase the amount of mirrors to reach the required power, which in turn would change the total efficiency of the field and this would change again the amount of heliostats and so on. Performing this process, after a few iterations, changes in overall efficiency and reflected area would begin to become irrelevant, indicating the end of the procedure.

When this process has been performed, heat generation is scaled by the mold of the annual average value of solar radiation. After that, the cycle calculations would be redone based on the monthly radiation values, using the same number of heliostats determined by the annual criteria to analyze the generation variation in each month.

Due to some limitations of the studied pre-project, it was considered that the heliostat positioning system was active, that is, it would be automatic and would move following the daily solar path and the annual solar declination, to optimize the radiation incident on the heliostats.

4. RESULTS AND DISCUSSION

4.1 Solar Radiation Data

Accessing the CRESESB database, there are values of three weather stations in the region of Grande Dourados, with few variations between them as can be observed in Figure 6. The graph shows the monthly variation of solar irradiation in the region. It can be observed that in the fall period there is a sharp fall in values, with a slight recovery during winter and reaching the highest levels in spring and summer mainly.

The difference between the high and low peak, which occur respectively in December and June, is more than 3 kWh/m², i.e. there is a halving of the energy availability from December to June in the region, which is observed on the sharp curve of the graph.

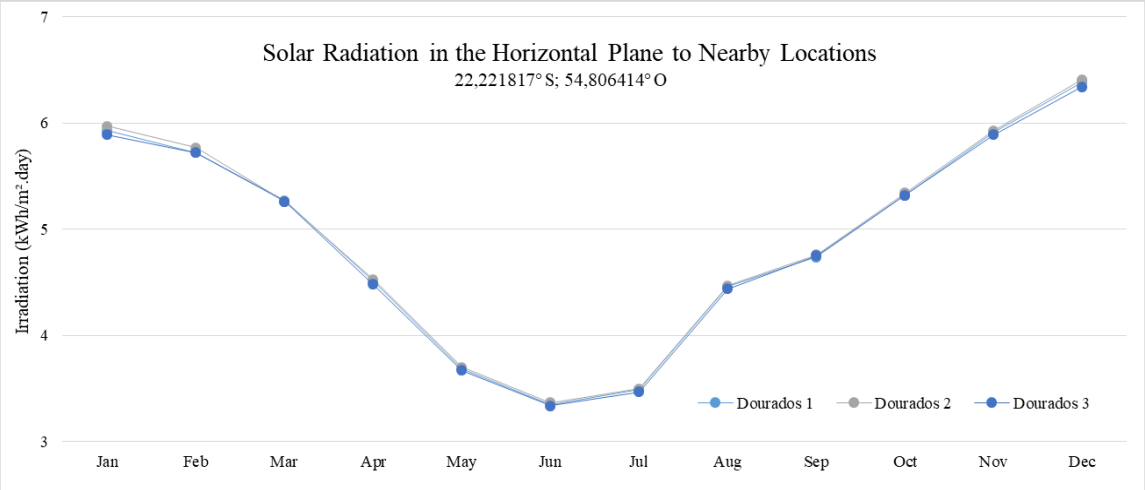

Figure 6. Monthly variation of solar irradiation in the region of Dourados. Source: CRESESB.

4.2 Distribution of Heliostats Field

Take into account the tower height of 120 m² and a heliostat dimension of 10 m x 10 m for the 100 m² surface, an approximate radial spacing (ΔR) value of 15 m and azimuthal spacing (ΔA) of 25 m (Eq.1-3).

The distribution needs to focus mainly as close as possible to the tower south. Following the average efficiency for cosine losses for certain areas of the heliostat field (Figure 5), we tried to focus as much as possible primarily on regions with efficiency of 90%, 87.5%, 85%, 80% and 70% respectively, respecting the maximum surfaces of each area, which is estimated with the known values of mirror dimensions and radial and azimuth distance (Eustáquio, 2011).

Therefore, the amount of heliostats distributed to each zone, following the efficiency distribution criterion due to cosine losses, follows in Tab. 1 below:

Table 1. Heliostat distribution.

Heliostat Field	
Nº Heliostats 90%	40
Nº Heliostats 87,5%	198
Nº Heliostats 85%	632
Nº Heliostats 80%	1005
Nº Heliostats 70%	765
Nº Total of Heliostats	2640

Considering the average efficiency by cosine effect (Figure 8), plus the attenuation efficiency calculated in *Excel* through Eq.4-5 and the other efficiencies (shading, blocking, reflectivity, blur, central receptor) that have average values established by Eustáquio (2011), a total heliostat field efficiency and overall efficiency are obtained, as shown in Tab. 2:

Table 2. Overall heat generation efficiency.

Overall Efficiency	
Cosine Effect (%)	79.0
Reflectivity (%)	90.0
Atmospheric Attenuation (%)	93.4
Shading (%)	97.0
Blocking (%)	97.0
Blurring (%)	90.0
Field Efficiency (%)	56.2
Tower Efficiency (%)	85.0
Overall Efficiency (%)	47.8

The Excel calculated result of 56.2% total heliostat field efficiency was close to the value of Eustáquio (2011) which reached a field efficiency of 63%, but with a lower number of 1263 heliostats against the 2640 heliostats in this work. When considering the efficiency of the central receiver, the overall efficiency of heat generation would be 47.8%.

4.3 Cycle Performance

Performing Rankine cycle calculations for the turbine inlet pressure and temperature conditions established in the selected steam turbine model (SIEMENS SST-300), the following results were obtained for the annual mean local radiation value (4.9 kWh/m²), presented in Tab. 3:

Table 3. Cycle performance (annual parameters).

Cycle performance	
Turbine Generated Power (MW)	18.6
Pump Consumed Power (MW)	2.4
Heat Generated Central Receiver (MW)	51.5
Condenser Withdrawal Heat (MW)	35.3
Net Power (MW)	16.2
Thermal Efficiency (%)	31.5

Presenting a net generated power of 16.2 MW, the cycle showed an expected result for generation (20 MW) considering that it has an average daily operating period of 12 hours. The flow rate established for the cycle was 17.3 kg/s so that it reached the inlet temperature of 520°C for a pressure of 120 bar and 51.5 MW heat generated in the tower for these average radiation conditions. , in order to reach an approximate value to what was expected.

Now calculating the results for monthly average radiation values, we will have a very high peak power variation, because the month with the maximum radiation month (December) has twice the energy availability of the month with the minimum (June). Figure 7 illustrates the relationship between the average irradiation of each month and the respective amount of heat generated:

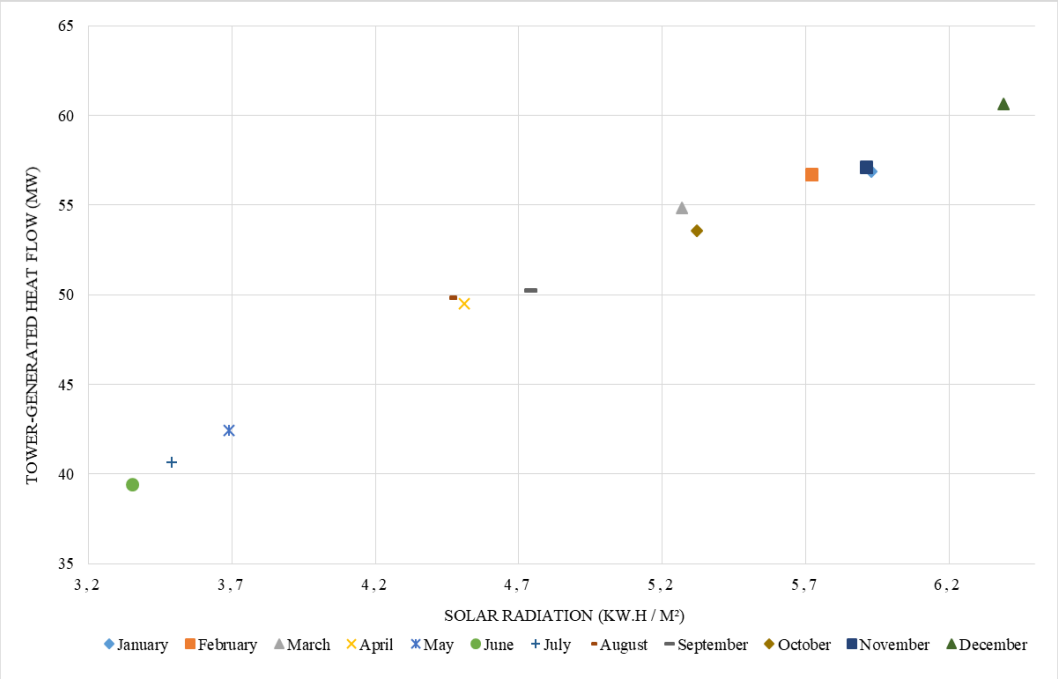

Figure 7. Solar Irradiation (kWh/m²) x Heat flux generated at Central Receiver (MW).

As can be seen, there is a difference of approximately 20 MW of power between the high and low radiation peak months in the region, which directly affects the power generated each month, which can be seen in Figure 8. It is observed that in November, December, January, February and March, which comprise the spring and summer periods in the south hemisphere, the desired power values of 20 MW are reached, while in the other months the values are below that mark. And on a similar curve follows the average thermal efficiency of the cycle monthly (Figure 9).

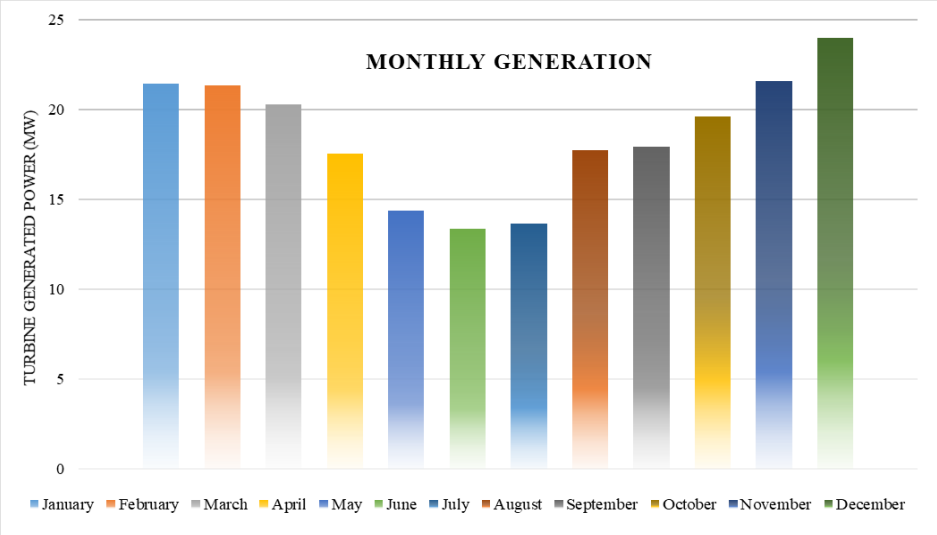

Figure 8. Monthly power generated in the turbine.

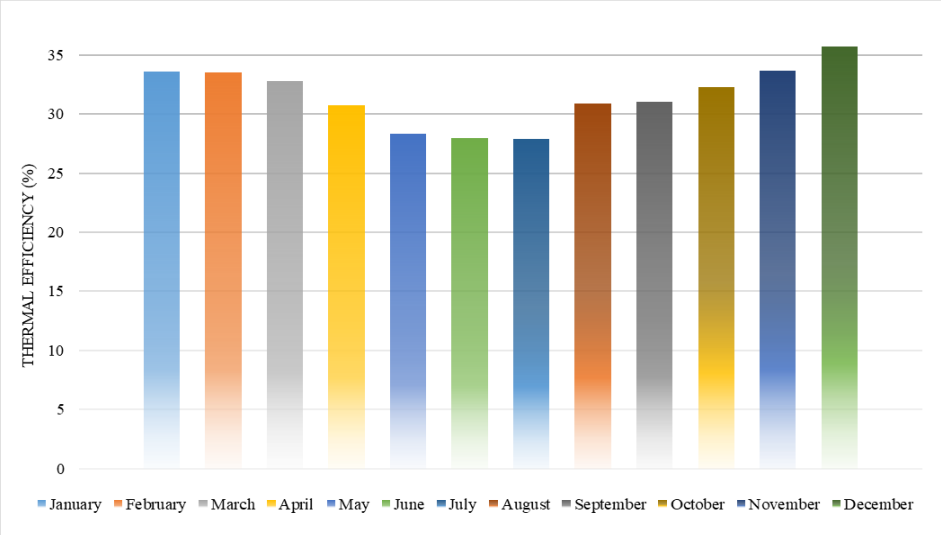

Figure 9. Monthly average thermal efficiency.

Although the curve is similar, it is less steep, following the trend that the higher the heat and power generation generated in the turbine, the higher the efficiency. However in this graph, the curve does not follow the same variation between the high and low peaks of the graph in Figure 8, in which case the variation between the high and low peaks is smaller. With thermal efficiency values ranging from 27% to 36%, the cycle has been shown to have a rate equivalent to conventional thermal power plant designs, whose cycles also have efficiency around 20% and 30% (Çengel and Boles, 2011). Remember that this efficiency is the cycle only, regardless of the efficiency of the heliostat field and the central receiver.

5. CONCLUSIONS

Despite the high oscillation in local solar irradiation rates, the region and also much of the country have great potential to exploit the various technologies of solar energy generation. Concentrated solar energy is still poorly studied and practically unexploited in Brazil, thus being a great waste of potential. Due to this, this paper aims to provide an initial result of a CSP system project.

The number of heliostats obtained for the approximate generation of 20 MW was more than double the result obtained by Eustáquio (2011), which shows that the issue of heliostat distribution and efficiency needs to be improved. Some alternatives would be to use smaller heliostats, thus reducing the radial and azimuth spacing and possibly increasing the mirrored area in the high efficiency cosine regions (Figure 5) and thus reducing the total field area.

The monthly generation values maintained the trend as a function of the month's average radiation, resulting in months of higher solar incidence with higher generation (above the 20 MW benchmark) and those of lower incidence with lower generation (below the 20 MW benchmark). This is due to the methodological choice of establishing the dimensions for the system as a function of the annual average radiation. Because of this, the generation continued according to the specific energy availability of each month. An interesting alternative to this methodology would be to establish a different heliostat cycle size and field pattern for each month, as the Grande Dourados region has a high variation during the year, thus optimizing generation during the year.

Another important point to note is that possible technical limitations of the turbine were not taken into account, because in some months of high incidence, the inlet temperatures would reach the order of 600°C and 700°C, values of supercritical cycles. Therefore, under these conditions turbines specifically designed to withstand such temperatures would be required.

In the work, several points to be improved are noticeable, such as the thermodynamic cycle itself and its type, the use of more efficient alternatives to the cycle such as molten salt, a thermal storage system and perhaps a better mirror distribution. The development of projects with other CSP technologies and their improvement, as well as developing them in specific software such as SAM and WinDelSol, are suggestions for future works subject.

6. ACKNOWLEDGEMENTS

Firstly, I thank to Professor Ramon Eduardo Pereira Silva for his guidance, teachings and support. I also thank the Energy Engineering course and UFGD for their support and the organization of COBEM 2019 for the opportunity.

7. REFERENCES

Aneel – Agência Nacional de Energia Elétrica. Chamada Nº 019/2015. Projeto Estratégico: "Desenvolvimento de Tecnologia Nacional de Geração Heliotérmica de Energia Elétrica". 1th May 2019 <http://www2.aneel.gov.br/arquivos/PDF/PD%20Estrategico%20019-2015.pdf>.

Badia, T. D., L'humanité entre en période de « dette écologique ». 10 Nov. 2018 <http://www.lemonde.fr/planete/article/2013/08/20/mardi- 20- aout- l- humanite- entre- en- periode- de- detteecologique_3463559_3244.html>.

Bezerra, H. S. "Energia Solar Concentrada: Simulação do Desempenho de Heliostatos de Pequeno Porte". UNESP. Botucatu, 2017. 27 May 2019. < https://repositorio.unesp.br/bitstream/handle/11449/152845/bezerra_phs_dr_botfca.pdf?sequence=3>.

SIEMENS. "Turbinas de Vapor Industriales". 20 Jan. 2019 <https://docplayer.es/23458690-Turbinas-de-vapor-industriales-la-gama-integral-de-productos-de-2-a-250-mw-answers-for-energy.html>.

Çengel, Y.A.; Boles, M.A. Termodinâmica. 7ª ed. São Paulo: McGraw Hill, 2013. 1048p.

CRESESB – Centro de Referências Solar e Eólica Sérgio de S. Brito. 27 May 2019. <http://cresesb.cepel.br/index.php#data>.

Eustáquio, J.V.C.S. 2011. "Simulação e análise do comportamento do campo de heliostatos de uma central de concentração solar termoelétrica de receptor central". Universidade do Porto. Porto, Portugal.

Farges, O. 2014. "Conception optimale de centrales solaires à concentration: application aux centrales à tour et aux installations beam down". Génie des procédés. Ecole des Mines d'Albi-Carmaux, Albi, France.

IEA – International Energy Agency. PVPS Annual Report: Implementing Agreement on Photovoltaic Power Systems. Photovoltaic Powers System Programme, 2017. 26 June 2019 <http://www.iea-pvps.org/fileadmin/dam/public/report/statistics/IEA-PVPS_-_Trends_in_PV_Applications_2017_-_EXECUTIVE_SUMMARY.pdf>.

Pereira, E.B., Martins, F.R., De Abreu, S.L., Rüther, R., 2017. "Atlas Brasileiro de Energia Solar/Brazilian Atlas of Solar Energy". 2º Edition. São José dos Campos, Brazil. 28 June 2019< http://ftp.cptec.inpe.br/labren/publ/livros/Atlas_Brasileiro_Energia_Solar_2a_Edicao.pdf>.

Portal Solar. "Energia Heliotérmica: Entenda como funciona". 06 May 2019. <https://www.portalsolar.com.br/blog-solar/energia-solar/energia-heliotermica-entenda-como-funciona.html>.

Shapiro, H.N.; Moran, M.J. Princípios de termodinâmica para engenharia. 7ª ed. Rio de Janeiro: LTC, 2009. 864p.

8. RESPONSIBILITY NOTICE

The author(s) is (are) the only responsible for the printed material included in this paper.